CHAPTER III

FAULTS IN INDUCTION MOTOR

3.1 INTRODUCTION

In Recent years, the problem of failure in large machine have become more significant and of concern in industrial applications. The desire to improve the reliability in industrial drive systems has led to researcha nd development activities in several countries to evaluate the causes and consequences of various faults. In particular ongoing research work is being focused on the causes of different faults and development of diagnostic tecniques for these faults.

The most prevalent faults in Induction Motor are briefly categorized as

- Rotor faults
- Bearing faults
- Eccentricity faults
- Stator faults

The surveys indicate that in general, failures in electrical machines are dominated by bearing and stator faults with rotor winding problems being less frequent. There can be significant variations on the above statistic, which will be unique to a particular group of induciton motors operating in a specific installations and is due to the numerous causes of failures.

The figure 3.1 shows the statistical spread in the various dominant failure mechanisms.

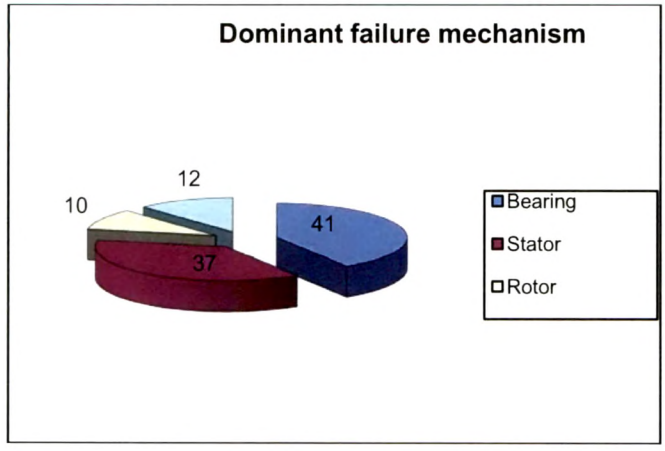

Figure 3.1: Different faults within Induction motors

3.2 Rotor faults

3.2.1 CAUSES OF ROTOR FAILURES

The majority of all rotor failures are caused by combination of various stresses like

- Thermal,
- Electromagnetic
- Residual
- Dynamic
- Mechanical
- Environmental

3.2.1.1 Thermal Stresses

3.2.1.1.1 Thermal Overload

Thermal overloading can occur during acceleration, running, or stall conditions. It should be kept in mind that some motors are stator limited and some are rotor limited from a thermal standpoint. While running at full load speeds, most motors

are stator limited. The stall condition has the greatest potential for rotor damage in the shortest time period and is the most difficult to protect against when relying on thermal protection

The most common causes of thermal overload failures are the following:

a) An abnormal number of consecutive starts, causing excessive bar temperature or end ring temperature

b) Rotor stalling due to high breakaway loading

c) Failure to accelerate to full speed due to intersect between the load and motor speed torque curve

d) The rotor rubbing the stator due to a bearing failure, rotor pull over, or abnormally high vibration

e) Unbalance phase voltages and corresponding negative sequence currents with associated rotor surface heating.

3.2.1.1.2 Thermal Unbalance

Thermal unbalance can be caused by either the effect of starting or running condition. Unbalance can also be inherently designed or manufactured into the rotor or can occur due to operation outside its design limits. The most common causes of thermal unbalance failures are the following.

a) Frequent starts causing temperature differential in the rotor bars due to the phenomenon of skin effect

b) Unequal heat transfer between the rotor bars and the rotor core.

c) The rotor bowing due to unequal changing of stacking pressures associated with thermal cycling

d) Loss of fit between the rotor core and the shaft due to the thermal expansion during startup, causing unstable vibration.

e) Hot spots on the surface of the rotor due to smeared lamination or rotor rubs

f) Temperature gradients due to unequal circulation currents. These can be generated by either broken and /or varying isolation or shorting of the rotor bars.

3.2.1.1.3 Hot spots and Excessive losses

There are number of variables during the manufacture, design or repair of rotor that can cause unpredictable losses and hot spots. Some of the variables that can cause these conditions are

a) Smearing of laminations in the slot or on the rotor surface

b) Irregular shorting of rotor bars to laminations in the slot area

c) Poor stacking of lamination: too loose, excessive burr, or lack of symmetry

d) Varying tightness of fit between rotor bar and lamination

e) Non uniform loss distribution in the lamination caused by improper annealing or insufficient control during lamination processing

f) Improper lamination design

g) Bad connections between bar to end ring

3.2.1.1.4 Rotor Sparking

There are several potential causes of rotor sparking on fabricated rotors. Some are of a non destructive nature, and some can lead to rotor failure. Non destructive sparking can and probably does occur during normal operation. This sparking is normally not observed due to its low intensity and /or the motor enclosures,

prohibiting its observance. Normal operation is defined as any motor that could be subjected to voltage dip, load fluctuation, switching disturbance, etc. Besides the aforementioned reasons, no sparking is usually observed during normal running at full load for several reasons. The centrifugal force at full load speed is usually greater than the electromagnetic forces acting on the bar due to rated current and tends to displace and hold the bar radially in the slot. Furthermore, the frequency within the rotor circuit is very low. This low frequency corresponds to a low impedance of the rotor cage circuit, essentially confining all rotor current to the cage itself. Therefore, although possible, no sparking is normally observed during normal operation at full load.

However during line starting, the current in the rotor cage is five to eight times normal. This high current combined with the higher cage impedance due to the frequency of the rotor current initially varying from line frequency at standstill, will cause voltage drop along the length of the bar in excess of eight times the normal running value. It is this voltage that tends to send current through laminations. In short, during startup, there are actually two parallel circuits- one through the rotor bar and the other through the laminations.

The design and manufacturing process for rotors include measures to reduce the sparking. However, material and manufacturing tolerances together with the effects of differential thermal expansion and thermal cycling preclude any motor from sparkless operation.

3.2.1.2 Electromagnetic Stresses

3.2.1.2.1 Electromagnetic Effect

The action of slot linkage flux, resulting from bar current, generates electrodynamic forces. These forces are proportional to square of rotor current and are unidirectional. They tend to displace the bar radially between the top and bottom of the slot. These forces vibrate the bar at twice the frequency of that of rotor current. Hence, they produce deflection or a bending stress in the bar. If the deflection is high enough, a fatigue failure in the bar will result. It can be shown that the radial force acting on the rotor bar will cause a deflection during startup that would be greater than that allowed by the normal slot confinement. It is theoretically proved that the bar actually flattens out in the center of the slot so that the stress at each end connector to bar joint is higher than that allowed by simple slot constrained bar motion.

3.2.1.2.2 Unbalance Magnetic pull

Unbalanced magnetic pull is a potential problem that can cause the rotor to bend and strike the stator winding. In the "ideal" motor, the rotor is centered in the air gap, and the magnetic forces are balanced in opposite directions causing no rotor deflection. In the real world, rotors are not perfectly centered in the air gap and things like eccentricity, rotor weight, bearing wear, belt loading and machine alignment all contribute to off centering of the rotor.

The air gap between rotor and stator decreases on one side while increasing on the other. In an alternating magnetic field, the result of a decreasing air gap is greater force of attraction across that gap, i.e. the reluctance of the flux path is reduced. The same magnetizing current in the winding can generate more flux across the gap, leading to still greater pull. At same time, the air gap is being increased on the

opposite side of the machine. Reluctance becomes greater there, so that flux and magnetic pull are reduced. Unbalance forces now act upon the rotor. The greater pull on the side having small gap will tend to move the rotor in that direction, making the gap still smaller. The process will continue until the gap becomes zero and the rotor comes into contact with the stator. The rotor bending is restrained by the stiffness of the shaft.

3.2.1.2.3 Electromagnetic noise and vibration

Air gap eccentricity can cause noise and vibration problems. The radial force produced by stator harmonics combine with those produced by the rotor harmonics can create electromagnetic noise and/or vibration. There are basic five types of air gap eccentricities that can occur

a) Rotor OD is eccentric to the axis of rotation

b) Stator bore is eccentric

c) Rotor and stator are round but do not have the same axis of rotation

d) Rotor and shaft are round but do not have the same axis

e) Any combination of the above is possible

These conditions may or may not cause a significant amount of electromagnetic noise or vibration.

3.2.1.3 Residual Stresses

These stresses can be present in any plane (i.e. radial or axial), and are normally not harmful to the rotor as long as they do not cause any significant change in the rotor geometry. Some of the more common residual stresses are the result of casting, brazing, welding, stacking and machining operations. On larger motors, it is common practice to relieve stress in the rotor shaft prior to final machining. If any of

these stresses do result in a change in the rotor geometry, they usually take place during the transition between idle and full load thermal conditions and can cause vibration problems, which might not be noticed while motor is running at no load.

4.2.1.4 Dynamic Stresses

3.2.1.4.1 Shaft Torques

The rotor is designed to handle torques in excess of that normally associated with motor full load or breakdown torque. Any torque above these levels is usually of short duration and referred to as a transient torque. Transient torques commonly occur on startup, bus transfers or out-of phase reclosures. They can also be generated by shock loading from driven equipment or by operation on an inverter power supply.

3.2.1.4.2 Centrifugal Forces

Normally a rotor is designed to be capable of being over speed within design limits. Even up to this speed, caution is necessary if the unit is energized during this condition. The reason for this caution is that components such as the rotor core to shaft interference fit are now required to handle both centrifugal as well as thermal stresses. If this fit is loose, then high vibration with corresponding destructive results might occur. Of course, centrifugal forces beyond the over speed limits also need to be checked for causing possible problem associated with end-ring or lamination stresses and /or retention of fan blades or balance weights.

3.2.1.4.3 Cyclic Stress

The motor shaft can be subjected to cyclic stresses that may lead to an eventual fatigue failure. Cyclic stresses can be caused by application, such as misalignment between drives equipment, over-tightened belts, or incorrect sheave size for overhung loads. Cyclic loads of this nature should be analyzed to make certain that safe operating limits are maintained.

3.2.1.5 Environmental Stresses

Foreign materials, which can cause abrasion or clog the ventilation paths, could constitute a stress, as could chemicals or moisture, which would attack and break down the basic rotor materials, A good example would be the high concentration of very caustic solution that would etch away an aluminum rotor cage or sulphur fumes, which could cause deterioration of the rotor brazing alloy. Motors with small gaps have actually had rotor rusts to the stator laminations when a large amount of moisture was present. Corrosion has also caused balance weights to come loose and "sling" into the stator winding with destructive results.

3.2.1.6 Mechanical Stresses

In addition to those failures associated with the previously mentioned stresses, there is another broad category of failures that can be grouped together under the general heading of mechanical failures. Some of the more common ones include the following

a) Casting porosity

b) Loose laminations

c) Broken parts

d) Incorrect fit between shaft and core

e) Poor rotor/ Stator geometry

f) Loss of air gap

g) Bent rotor shaft

h) Bearing failure

i) Misalignment

j) Tooth resonance

3.2.2 Fault modeling and Analysis

Whenever there is fault in bar, the current in bars redistributes itself. Figures 3.2 shows the redistribution of current in a rotor with a single bar at the instant when the sinusoidal current envelope is near to its maximum value at the position of the broken bar. The current redistributes itself in the surrounding bars. Most of current that would have flowed in the broken bar now flows in the two bars immediately adjacent to it on either side.

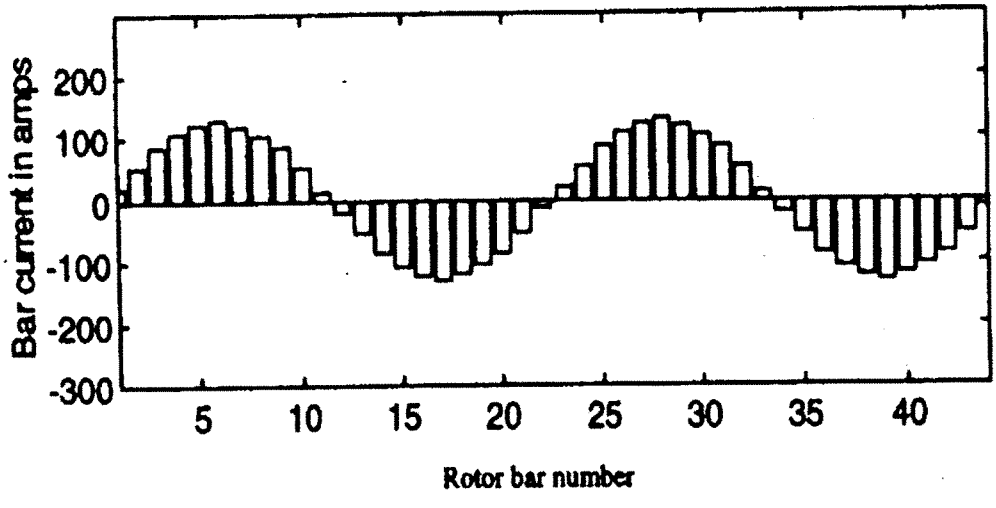

Figure 3.2: Rotor bar current distribution before fault

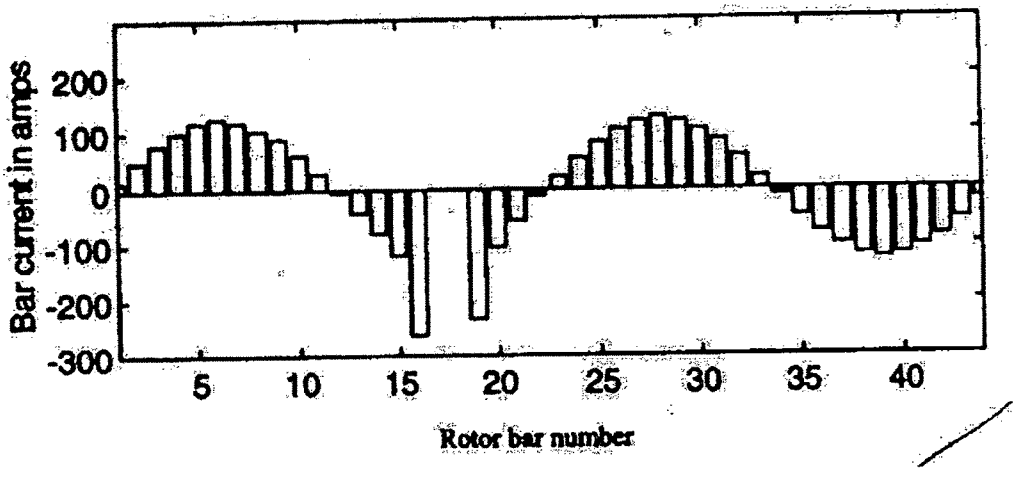

Figure 3.3: Rotor bar current distribution after fault

To model a particular broken bar, it is assumed that the fault current is equal and opposite of the normal current flowing through the healthy bar. When normal and fault currents are superimposed, the current pattern depicted in figure 3.3 is obtained. To solve for the magnetic field in the air gap under the fault condition it is sufficient to find the fields that are caused only by the fault current.

Each individual rotor bar can be considered to form a short pitched single turn, single-phase winding. The air gap field produced by a slip frequency current flowing in a rotor bar will have a fundamental component rotating at a slip speed in the forward direction with respect to rotor and one of equal magnitude that rotates at the same speed in the backward direction. With symmetrical rotor, the backward component sums to zero. For a broken bar rotor, however the resultant is non-zero. The field, which rotates at slip frequency backward with respect to the rotor, will induce EMF on stator side that modulates the main frequency component at twice slip frequency.

3.2.2.1 Fundamentals on Twice Slip Frequency Side bands

The General equation that relates the supply frequency (f_1) of the voltage supply to a three phase stator winding, the synchronous speed (N_s) of the rotating magnetic filed produced by the stator winding, and (p) the pole pairs of th winding is given by

$$f_1 = N_s * p \qquad (3.1)$$

Under perfectly balanced conditions then only a forward rotating field is produced, which rotates at synchronous speed. The rotor rotates at Nr and rotor always rotates at a speed less than the synchronous speed, A of measure of the slip in back of the rotor is termed as slip, defined as

$$s = (N_s - N_r)/ N_s \qquad (3.2)$$

The slip speed (N_s-N_r) is the actual difference in rpm between the speed of the rotating magnetic field and the actual speed of the rotor, but note that the slip frequency is not the slip speed divided by 60. The term slip frequency has a specific definition. The frequency of the rotor currents is termed as slip frequency and is derived as follows

$$f_2 = (N_s - N_r)*p = s * N_s *p = s*f_1 \qquad (3.3)$$

Under normal operation, the rotating magnetic field produced by the currents flowing in the rotor conductors moves faster than the actual rotor speed Nr ($N_2 = N_s$-N_r)

Now the speed of the rotating magnetic field produced by the current carrying rotor conductors with respect to the stationary stator windings is given by

$N_r+N_2 = N_r+N_s - N_r = N_s$ (3.4)

With respect to the stationary observer on the fixed stator winding, then the speed of the rotating magnetic field from the rotor equals the speed of the stator rotating magnetic field i.e N_s . Both fields are locked togather to give a steady state torque production by the induction motor.

With broken bars, there is an additional rotating magnetic field produced. Broken rotor bars produce a backward rotating field N_b at slip speed(-ve direction $(N_s-N_r) =sN_s$) with respect to the rotor.

$N_b = N_r - sN_s = N_s (1-s) - sN_s = N_s -2sN_s$ (3.5)

The stationary observer on the stator winding now sees a rotating field at ,

$N_b= N_s (1-2s)$

Expressed in terms of frequency, speed of rotating magnetic field and number of pole pairs this gives

$f_b= (N_s (1-2s))*p = (f_1/p(1-2s))*p = f_1(1-2s)$ (3.6)

The side band components around the fundamental of the line current spectrum are usually measured, detecting broken bar faults given by

$$f_b = (1 \pm 2s) f \quad \text{Hz} \qquad (3.7)$$

In fact the analytical expression for the frequencies that are present in the air gap flux is given by

$$f_k = f\left[\left(\frac{k}{p/2}\right)(1-s) \pm s\right] \qquad (3.8)$$

Where

f = Line frequency; k = Harmonic index ; P = no. of poles ;

s = slip

All of these frequencies should be present in the air gap flux. Rotor quality, cage misalignment, variation of cage conductivity, bearing misalignment and magnetic orientation of the laminations may create air gap disturbance which, as far as its fundamental field is concerned, cannot be distinguished from the broken bar effects. While it cannot reliably be established the presence of broken bars based solely on the low frequency spectra, the high frequency content of such a disturbance provides an opportunity for an unambiguous decision. Figure 3.4 shows the comparison of air gap flux density spectra for various asymmetries to those predicted for a single broken bar in the same machine.

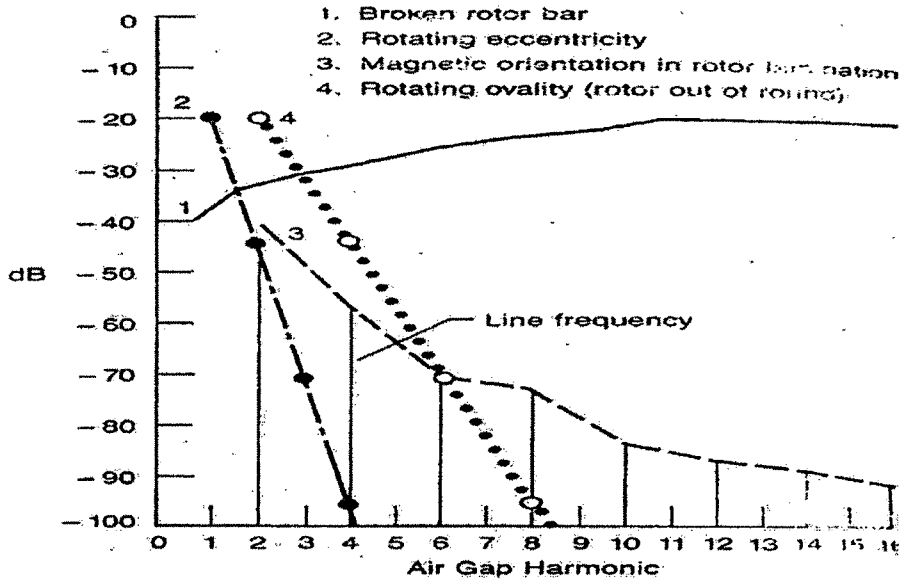

Figure 3.4: Comparison of air gap flux spectra for single broken bar and various asymmetries in the same motor

Two important features in figure 3.4 should be noted

3.3 The magnitude of the line frequency sidebands due to asymmetries may be comparable to or larger than those due to a broken bar in the same motor

3.4 The magnitudes of the asymmetry components decay much more rapidly, in the higher harmonics, than those for a broken bar.

The first conclusion to be drawn is that there is real possibility that, with sufficient sensitivity to detect a single broken bar, manufacturing or other asymmetries may give rise to a false broken bar indication. The second conclusion that may be drawn is that by examination of the higher harmonic amplitudes asymmetries may be distinguished from broken bars.

The amplitude of the air gap flux harmonics at the frequencies given by above equation are controlled by the rotor parameters that are collectively referred to as the "cage magnetic Reynolds number" or "Motor goodness factor ".

Due to structure of the windings in a motor only those frequency where k/p= 1,5,7,11,13 .... etc will in theory appear.

So substituting K/p =1,5,7,.... and fundamental frequency f = 50 Hz the predictable frequency appearing in the spectral plots will be as per the table 3.1

Table 3.1: Predictable Frequency for Rotor Faults

Nomenclature	Frequency (Hz)
Fundamental	50
LSB1 (lower side band 1st harmonic)	50*(1-2s)
USB5 (Upper side band 5th harmonic)	250*(1-4s)
LSB5 (lower side band 5th harmonic)	250*(1-6s)
USB7 (Upper side band 7th harmonic)	350*(1-6s)
LSB7 (lower side band 7th harmonic)	350*(1-8s)

3.2.2.2 Motor current slip ratio amplitude

All motors under load, develop slip. Slip is difference between the actual rotating speed and the synchronous speed of the motor. If there is a condition in the motor circuit that creates a high resistance, e.g broken bars, loose joints etc. then the slip frequency will be seen in the spectrum. The measure of the resistance in the motor circuit can be determined by measuring the difference in amplitude of the line frequency and slip frequency and calculating db ratio

20 log (A/B), where A = Slip frequency Amplitude/ LSB1 (3.9)
B = Line frequency Amplitude / Fundamental

From the Experimental results it was observed that if the ratio of slip frequency amplitude to the line frequency amplitude is greater than 45 db, the resistance in the bars is normal i.e. no fault exists. If it is between 40 db and 45 db, there is probably a source of high resistance/ fault developing. Below 40 db there is definitely a problem and as the ratio decreases it is a measure of increasing resistance.

To verify the above developed equation, the experiment was carried out using the induction motor directly fed from normal 3ph supply. The motor was first loaded with healthy rotor till its rated load and the measurements of no load losses, load current speed was carried out. The current signature was also recorded using the oscilloscope and inbuilt FFT programme. The magnitude of Lower side band LSB1 was measured from the oscilloscope and then converted to %. The motor current slip ratio amplitude in db was then measured using the equation mentioned in (3.9)

The same experiment was repeated with the one bar of rotor in crack condition. The crack in the rotor bar was carried out by drilling in the joint between end ring and rotor bar. The same measurement mentioned above were carried out. The experiment was continued for two bar and three bar failure. The results of the same are tabulated in table 3.2

Table 3.2 : Experimental results with rotor faults

Sr. no.	Particulars	W/o fault	One bar failure	Two bar failure	Three bar failure
1	No load current, A	0.813	0.916	0.916	0.94
2	Constant losses, w	129.5	160.5	170.3	178.5
3	Load current, A	1.71	1.7	1.91	2.06
4	Speed, rpm	2825	2825	2797	2758
5	LSB1, %	0.36	2.7	3.3	4.36
6	Motor current slip ratio amplitude, db	48.8	31.2	29.5	27.2
7	Starting current, A	10.4	10.3	12.4	17
8.	Efficiency, %	73.4	71.24	68.6	66.4

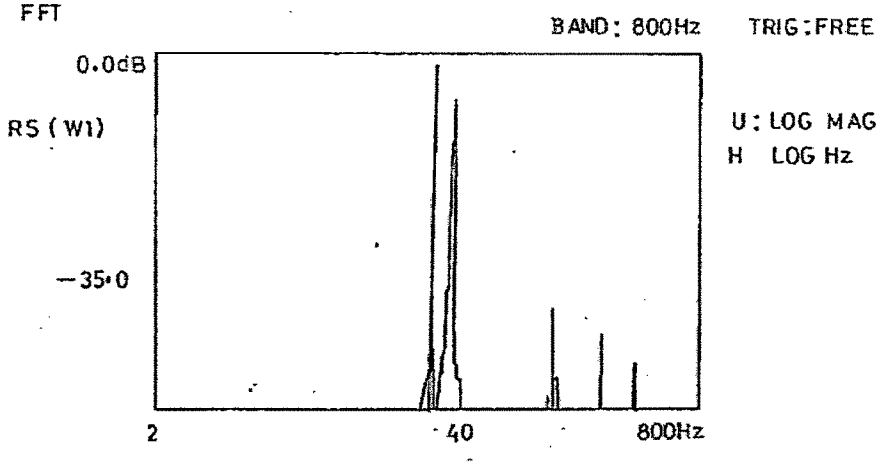

Figure 3.5: Oscillogram with no rotor fault

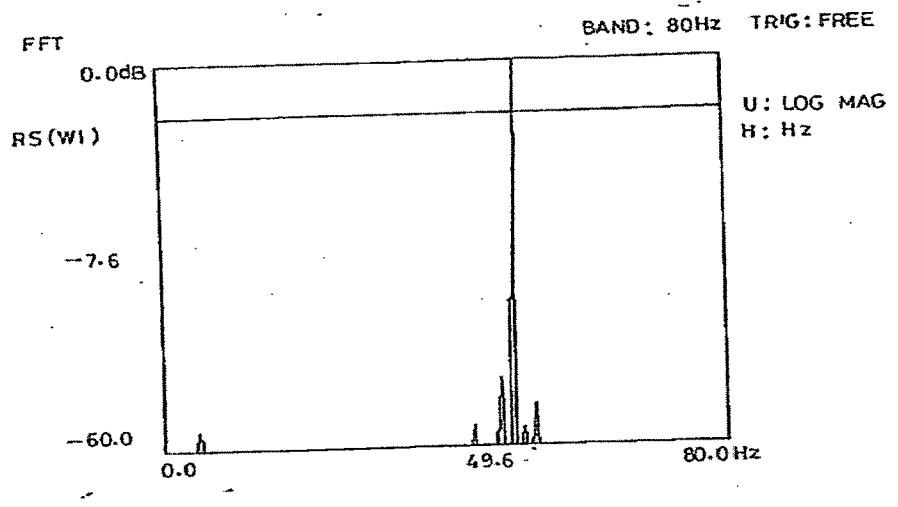

Figure 3.6 Oscillogram with one bar failure

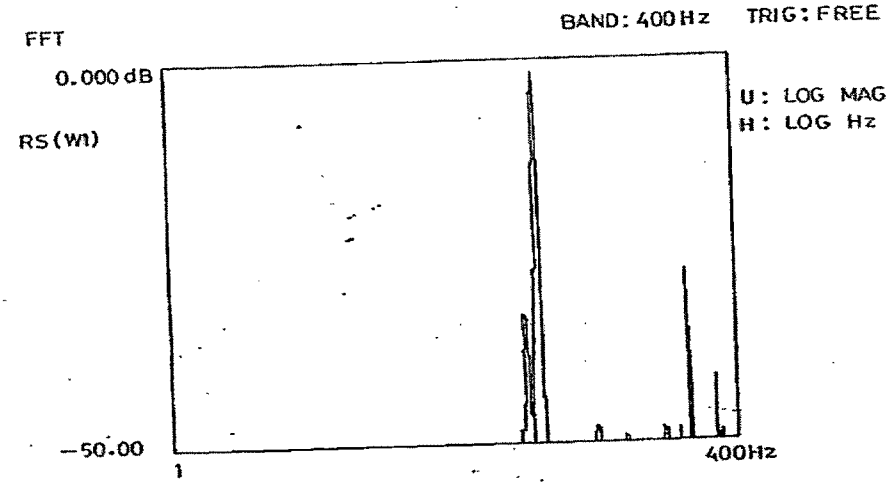

Figure 3.7: Oscillogram with two bar failure

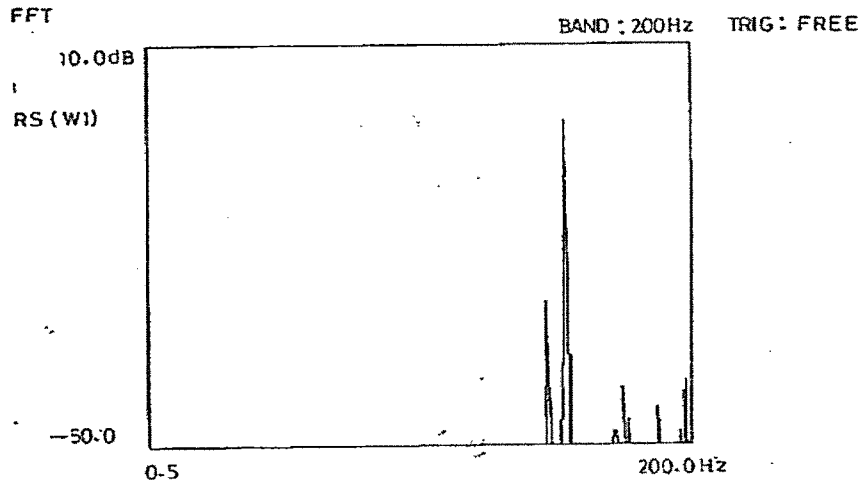

Figure 3.8: Oscillogram with three bar failure

3.2.3 Results & Discussion

From table 3.2 it can be seen that with no broken bars there is appearance of lower side band LSB1 but the magnitude is very less and the ratio of slip frequency amplitude to line frequency amplitude is around 48 db i.e. greater than 45 db and the signature in the figure 3.5 shows the lower magnitude of LSB1. hence no fault exists within the rotor.

With one broken bar, there is increase in the magnitude of LSB1. The ratio also drops down to 31 indicating the fault within rotor. The constant losses and no load current of the motor also increase. There is also decrease in the efficiency of the motor. The figure 3.6 shows the increase in the magnitude of LSB1 to the tune of 2.7% from 0.36%

With increase in the bar failure there is increase in magnitude of LSB1 and ratio and efficiency goes on decreasing. The slip, constant losses and no load current go on increasing. Figure 3.7 & 3.8 shows the further increase in the magnitude of LSB1 to maximum of 4.36%. This shows that equation (3.9) can be used to identify and quantify the extent of rotor failures.

So also to cope with low full load slips, there should be good FFT resolution, of order about 0.01 Hz. The detection of twice slip frequency side band on no load is not possible since the current in the rotor bars in negligible.

3.2.4 Effect of Time varying loads on Rotor Detection

While these detection have been shown to work, they assume that the load torque does not vary with rotational speed. If the load torque varies with rotor position, such as with a reciprocating compressor, then the current contains spectral components which coincide with those caused by a fault condition. This situation complicates any proposed fault detection scheme.

A large number of induction machine faults can be divided into two categories those that affect the air gap permeance (P_{ag}) or those that affect the air gap MMF (MMF_{ag}). Variations in either of these categories affect the mutual and self inductance of the motor, giving rise to detectable changes in stator current spectrum. These changes can , however, be obscured by the currents produced by position varying load torque, such as that of reciprocating compressor.

Variations in the machine's air gap are caused by such factors as rotor unbalance, rotor and stator slots, and mechanical motion between stator and rotor. These non

uniformities can be modeled by the machine's air gap permeance [36] as a Fourier series of sinusoidal functions dependent upon the stator angular position, ϕ_s and the mechanical rotor position with respect to the stator, θ_{rm}. In particular, a dynamic rotor eccentricity can be expressed as series of sinusoidal functions by

$$P_{ag}(\phi_s, \theta_{rm}) = \sum_{n=0}^{\infty} PnCos\{n(\phi s - \theta rm)\} \quad (3.10)$$

Variation in the air gap MMF, such as broken rotor bars or non sinusoidal winding distributions, can also be modeled with Fourier Series. In the ideal Induction Motor, the stator windings are assumed to b sinusoidally distributed, causing the stator flux to be purely sinusoidal.

Because the air gap flux density is defined to be the product of the air gap MMF and the air gap permeance

$$B_{ag}(\phi_s, \theta_{rm}) = MMF_{ag}(\phi_s, \theta_{rm}) * P_{ag}(\phi_s, \theta_{rm}) \quad (3.11)$$

Anomalies in either the permeance or the MMF will produce sinusoidal variations in the air gap flux density which is determined by the product of the two series. The mutual inductance of an induction machine is calculated by summing the flux linking each turn of the winding and dividing by the current that produces the air gap flux i_{mmf} [19]

$$L(\theta_{rm}) = \frac{\int Nw(\phi s, \theta rm)[\int Bag(\phi s, \theta rm) * r * l * d\phi s] d\phi s}{immf} \quad (3.12)$$

Where N_w is the winding distribution, and r & l represent the av. Air gap radius and the axial length of the air gap, respectively. The self inductance is calculated in the same way except that it includes a constant term to account for the winding leakage flux. Since the machine inductances are computed directly from the air gap flux density, any sinusoidal variation in the air gap permeance or the air gap MMF will cause the inductances to vary with respect to the mechanical rotor posistion θ_{rm}, or the mechanical rotational speed of the motor f_{rm}, in Hz

The voltage equation modeling an ideal induction machine in the arbitrary reference frame, assuming no neutral connection is

$$v_{qs} = R_s * i_{qs} + \omega\lambda_{ds} + d(\lambda_{qs})/dt \qquad (3.13)$$
$$v_{ds} = R_s * i_{ds} + \omega\lambda_{qs} + d(\lambda_{ds})/dt$$
$$0 = R_r * i_{qr} + (\omega - \omega_r)\lambda_{dr} + d(\lambda_{qr})/dt$$
$$0 = R_r * id_r - (\omega - \omega_r)\lambda_{qr} + d(\lambda_{dr})/dt$$

Where vqs & vds are the stator voltages, R_s & R_r are the stator and rotor resistances, i_{qs}, i_{ds}, i_{qr}, i_{dr} are the stator and rotor currents, ω is the reference frame angular velocity, and ωr is the electrical rotor angular velocity. The stator and rotor flux linkages are given by

$$\lambda_{qs} = (L_{ls} + L_m)i_{qs} + L_m i_{qr} \qquad (3.14)$$
$$\lambda_{ds} = (L_{ls} + L_m)i_{ds} + L_m i_{dr}$$
$$\lambda_{qr} = (L_{lr} + L_m)i_{qr} + L_m i_{qs}$$
$$\lambda_{dr} = (L_{lr} + L_m)i_{dr} + L_m i_{ds}$$

Where L_{ls} & L_{lr} represent the stator and rotor leakage inductances and L_m represents the mutual inductances.

To the stationary reference frame ($\omega = 0$), if the stator voltages vary sinusoidally and the stator copper losses are neglected, then it can be seen from the above equation, that the stator flux linkages oscillates at the electrical supply frequency, f. Since the stator flux linkages vary at a single frequency, above equation shows that any oscillations in the mutual inductances at rotational speed will result in stator current spectral components at frequencies $f \pm f_{rm}$. In practice, the stator current will contain components at $f \pm$ mfrm due to the interaction of the machine fluxes, torque and load.

Air gap eccentricities which vary at multiples of the mechanical rotor position will give rise to stator current spectral components at frequencies given by

$$f_{ecc} = f \pm m f_{rm} \qquad (3.15)$$

Anomalies in the air gap MMF will also generate stator currents in the same fashion. A broken rotor bar will produce spectral components defined by

$$f_k = f\left[\left(\frac{k}{p/2}\right)(1-s) \pm s\right] \qquad (3.16)$$

By comparing the frequencies generated by above eqn. (3.15) & (3.16), it is clear that many of the same current components are excited by different fault conditions.

The stator current is affected by load torque oscillations in a way similar to that explained above. In the sinusoidal steady state, it is clear that load torque oscillations produces an oscillation in the developed torque T. Therefore, since the mechanical system is assumed linear, the torque developed by an induction motor contains all the frequency components of the load torque. The magnitude of the developed torque harmonics are primarily dependent on the system inertia. The

electromagnetic torque can be expressed as the interaction of the stator flux and the stator current

$$T = 1.5p(\lambda_{ds} * i_{qs} - \lambda_{qs} * i_{ds}) \qquad (3.17)$$

In an ideal machine where the stator flux linkage is purely sinusoidal, any oscillations in the load torque at a multiple of rotational speed (mfrm), such as reciprocating machines will produce stator current at frequencies of

$$f_{load} = f \pm mf_{rm} = f\left[\left(\frac{m}{p/2}\right)(1-s) \pm 1\right], \qquad (3.18)$$

where m= 1,2,3.... Since the same frequencies are given by equation (3.15) & (3.16), it is clear that when the induction machine operates with a typical position varying load torque, the torque oscillations results in the stator currents that can obscure and often overwhelm, those produced by the fault condition.

This clearly has important impact on the formulation of an online failure prediction scheme. Common prediction scheme are based on the lowest harmonic component produced by a fault since this component is largest and therefore easiest to measure. Several approaches to online fault detection can be taken depending on the nature and user knowledge of the load torque. In the case where the load torque is know to contain only specific harmonic components, the stator current harmonics which are not affected by the load should be monitored. For example, a typical two cylinder compressor only contains even harmonics of the rotor speed. Therefore, stator current harmonics corresponding to the odd values of m in (3.18) can be monitored for fault effects. Examination of (3.16) shows that the first harmonic associated with a broken bar corresponds to a load torque harmonic at 2(p/2) times the rotational

speed. Clearly, then broken bars can be easily detected if the load torque does not contain the pth harmonic.

The impact of the load on a fault detection scheme is also dependent on the mechanical system inertia. In many cases, the load oscillation are heavily damped in the developed torque due to high inertia. In this situation, adequate detection can be accomplished by monitoring fault frequencies at sufficiently high harmonics. In the case of a broken bar fault, this effect is especially pronounced. The broken bar harmonics decay very slowly in magnitude as function of harmonic number. The lowest harmonic produced by the broken bar coincides with the pth harmonic of the torque, where p is number of poles. Therefore in many operational situations, where the system inertia is large, the lowest harmonic associated with the broken bar is often sufficient for fault detection. Furthermore, if the load torque is damped only at frequencies higher than m = p, then the broken bars can be detected from the higher order broken bar induced harmonics. There is, however a practical limit to higher harmonic detection since the current components of the interest with the fault are typically 40-50dB below the fundamental for the lowest harmonic. Measurement of the higher harmonic components greater than the 4^{th}, is generally not possible

The effect of load oscillations on the detection of rotor eccentricities and electrical unbalance is more acute. It is due to the fact that the harmonic magnitudes drop off much more rapidly as of function of harmonic number. This is true since the fault effect is more nearly sinusoidal. In this case, knowledge of load spectra content and inertial damping is required in order to avoid the effected harmonics. Additionally, rotor eccentricities and unbalances can easily occur in smaller machines with low inertia , while broken bars most often occur in large machines.

3.2.5 Effect of Speed Fluctuation, inertia

There are a lot of factors affecting the fault characteristics, such as speed fluctuations, inertia etc, if these factors are not studied, the accuracy of fault diagnosis will be seriously affected.

When symmetrical stator windings are connected into symmetrical three phase alternating electrical source, a revolving magnetic field with frequency f will be generated. This revolving magnetic field will produces emf with frequency of sf in the rotor winding. For a rotor winding fault machine, because of the asymmetric of the rotor, rotor current generates two revolving magnetic field as explained earlier with the same magnitude and reverse direction, their frequencies are ±sf(in reference to rotor), the +sf component interact with stator current magnetic field ; while the –sf component produces emf with frequency of (1-2s)f in stator winding, generating corresponding current. This extra current component (I_{2s}) balances with the –sf current component in rotor. The instantaneous value of the component with the frequency of (1-2s)f in stator current is

$$i_{2s} = I_{2s} \cos[(1-2s)\omega t - \acute{\alpha}_{2s}] \qquad (3.19)$$

This current interacts with fundamental wave flux $\psi\cos(wt - \acute{\alpha}\psi)$, generating fluctuation torque with frequency 2sf;

$$\Delta T(t) = 3P\psi I_{2s} \sin[2s\,\omega t - (\acute{\alpha}_{\psi} - \acute{\alpha}_{2s})] \qquad (3.20)$$

The relative value of fluctuation Torque is

$$T_{pul} = \Delta T/T = \frac{3P\psi I2s}{3P\psi I2s\sin(\acute{\alpha}\psi 1)} \approx I_{2s}/\,I\cos\phi \qquad (3.21)$$

Where T is steady state torque, I is the magnitude of stator current fundamental wave, because

Jd ω_r /dt = $\Delta T(t)$, where J is inertia,

It can be seen, the fluctuation of the torque will certainly lead to the fluctuation of rotating speed $\Delta\omega_r(t)$, its fluctuation frequency is also 2sf.

Its relative value is

$$\omega_{pul} = \Delta\omega_r / \omega_r = \Delta T / J2s\omega\omega_r = PT\, I_{2s} / J2s\omega\omega_r I\cos\phi \qquad (3.22)$$

Because of the fluctuation of rotating speed, there appears three frequency components in the induced emf in stator winding, they are the fundamental wave and the superimposed components with frequencies of (1±2s)f caused by rotor speed fluctuation.

The two induced emf with frequencies of (1±2s)f are same in magnitude, both superimposed on the fundamental emf. The one with the frequency of (1-2s)f generates current I'_{2s}, this current interacts with the first current component I2s, with frequency (1-2s)f (this component is not caused by speed fluctuation).

Another component of emf with the frequency (1+2s)f generates current I''_{2s}. This current generates magnetic field with frequency 3sf (relative to rotor), because of the asymmetry of the rotor, the corresponding emf produce current, forming two revolving magnetic field with frequency ±3sf. This phenomenon continues, producing a series of current components with the frequencies of (1±2ks)f, because

the components of the first sideband is larger (k=1), the study is mainly focused on this sideband.

As for magnitude, machine's functions on speed fluctuations on speed fluctuation caused by either I'_{2s} current component or I''_{2s} current component are the same. It means I'_{2s} equals I''_{2s} in magnitude, thus numerically I'_{2s} can be replaced by I''_{2s}

In another aspect, (1-2s)f component in stator current has two sources; one is the I_{2s} caused by revolving magnetic field and asymmetry of rotor winding(not considering speed fluctuations), another is I'_{2s} caused by speed fluctuation. So the (1-2s)f component we measure actually is total (1-2s)f component, i.e the sum of the above two component. Its magnitude is the minus of the two

$$i_{2s} + I'_{2s} = (I_{2s} - I'_{2s})\cos[(1-2s)\,\omega t - \acute{\alpha}_{2s}] \qquad (3.23)$$

Based on the above analysis, it can be concluded that (1-2s)f component in I_{2s}, in stator current is caused by asymmetry of the rotor, cause speed fluctuation, this fluctuation generates I'_{2s} and I''_{2s} two current components, the magnitude of these two components are approximately the same. The actually measured (1-2s)f component is the result of the interaction between I_{2s} and I'_{2s}, its value if different from either I_{2s} or I'_{2s}. The measured value of (1+2s)f can be used to correct fault characteristics of rotor winding, that is to add (1-2s)f measured value($I_{2s} - I'_{2s}$) with (1+2s)f measured value I''_{2s}, the result is taken as the actual fault characteristic.

According to the above analysis, after torque fluctuations caused by rotor winding fault, because the inertia is not infinite, the rotor speed fluctuation with twice slip frequency will be generated. thus the change the fault characteristic

From equation (3.22) , it can be seen, when inertia is large, the speed fluctuation is small, its impact on the fault characteristic in stator current is small; whereas when inertia is small, the speed fluctuation is large, its impact on the fault characteristic in stator current is also large. When load inertia decrease, (I_{2s} - I'_{2s}) will drop, but I''_{2s} will increase. Hence I''_{2s} is used to correct (I_{2s} - I'_{2s}), This helps to eliminate the effect of load inertia on fault characteristics.

3.3 Bearing Faults

3.3.1 Bearing failure causes

Rolling element bearings generally consist of two rings an inner and outer, between which a set of balls or roller rotate in raceways. Under normal operating conditions of balanced load and good alignment, fatigue failure begins with small fissures, located below the surfaces of the raceway and rolling elements, which gradually propagate to the surface generating detectable vibrations and increasing noise levels. Continued stressing causes fragments of the material to break loose producing a localized fatigue phenomena known as flaking or spalling. Eventually failure results in rough running of the bearing. While this is normal mode of failure in rolling element bearings.

The external source includes contamination, corrosion, improper installation or brinelling. Contamination and corrosion frequently accelerate bearing failure because of harsh environment present in most industrial settings. Dirt and other foreign matter that is commonly present often contaminate the bearings lubrication. The abrasive nature of these minute particles whose hardness vary from relatively soft to diamond like , cause pitting and sanding action that give way to measurable wear of the balls and raceways

Bearing corrosion is produced by the presence of water, acids, deteriorated lubrication and even perspiration from careless handling during installation. Once the chemical reaction has advanced sufficiently, particles are worn off resulting in the same abrasive action produced by bearing contamination.

Installation problems are often caused by improperly forcing the bearing onto the shaft or in the housing. This produces damage in the form of brinelling or false brinelling of the race ways which leads to premature failure. Misalignment of the bearing, which occur in the four ways depicted in figure 3.9 is also common result of defective bearing installations. The most common of these is caused by tilted races.

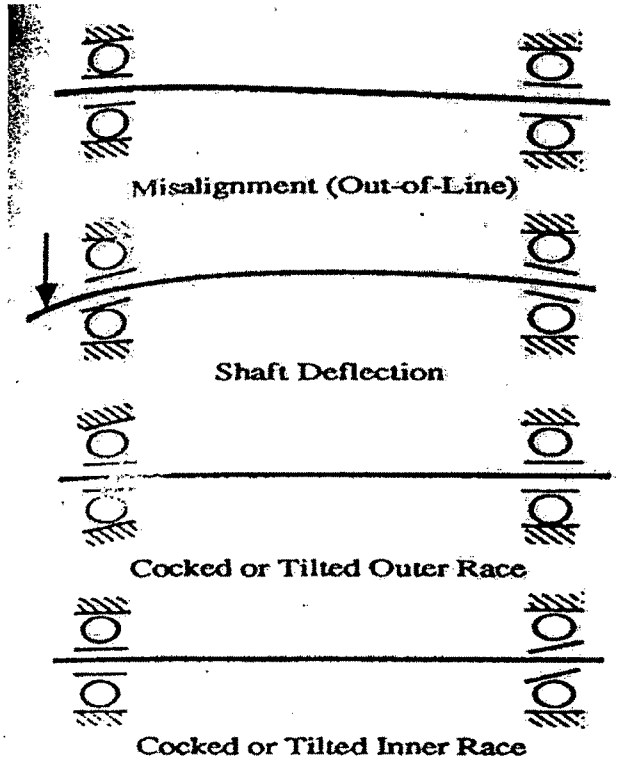

Figure 3.9: Types of Rolling element bearing Misalignments

Brenilling is the formation of indentations in the raceways as a result of deformation caused by static overloading. While this form of damage is rare, a form of false brenilling occurs often. In this case, the bearing is exposed to vibrations while stationary. Even though lightly loaded bearings are less susceptible, the false brinelling still happens and has even occurred during the transportation of uninstalled bearings.

Regardless of failure mechanism, defective rolling element bearing generate mechanical vibrations at the rotating speed of each component. These characteristics frequencies which are related to the raceways and the balls or can be calculated from the bearing dimensions and the rotating speed of the machine. Mechanical vibration analysis techniques are commonly used to monitor these frequencies in order to determine the condition of the bearing.

3.3.2 Diagnosis of Bearing faults

The relationship of the bearing vibration to the stator current spectrum can be determined by remembering that any air gap eccentricity produces anomalies in the air gap flux density. Since ball bearings support the rotor, any bearing defect will produce radial motion between the rotor and stator of the machine. The mechanical displacement resulting from the damaged bearing causes the air gap of the machine to vary in the manner that can be described by a combination of rotating eccentricities moving in both directions i.e clockwise and counterclockwise. As with the air gap eccentricities, these variations generate stator current at predictable frequencies. F_{bng}, related to the vibrational and electrical supply frequencies by [26]

$f_{bng} = [f_e \pm mf_v]$, where m = 1,2,3 ... and f_v is one of the characteristics vibration frequencies. (3.24)

The characteristic frequencies for ball bearings are based upon the bearing dimensions shown in figure 3.10.

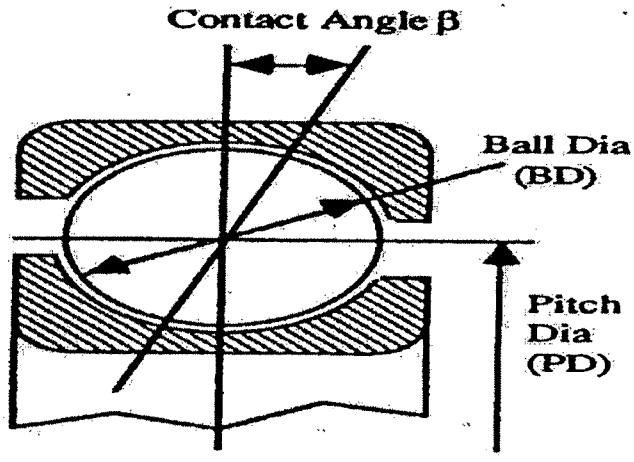

Figure 3.10: Ball Bearing Dimensions

In radially loaded bearings, the contact areas of the balls and raceways carry the heaviest loads causing most fatigue failures to involve these components. The ball spin frequency is caused by the rotation of each ball about its center. Since a defect on a ball will contact with both inner and outer races during every revolution, the ball defect frequency is twice the spin frequency and can be written as

$$f_b = \frac{PD}{BD} f_{rm}\left[1-\left(\frac{BD}{PD}\cos\beta\right)^2\right] \text{ Where} \qquad (3.25)$$

PD is the bearing pitch diameter, BD is the ball diameter, Beta is the contact angle of the balls on the races, and f_{rm} is the mechanical rotor speed in Hz. The outer and

inner raceway frequencies are produced when each ball passes over a defect. This occurs n times during complete circuit of the raceways where n is number of balls. This causes the outer and inner race frequencies to be defined as

$$f_o = \frac{n}{2} f_{rm}\left[1-\left(\frac{BD}{PD}\cos.\beta\right)\right] \qquad (3.26)$$

$$f_i = \frac{n}{2} f_{rm}\left[1+\left(\frac{BD}{PD}\cos\beta\right)\right]$$

Bearing cage faults generally bind the balls producing skidding and slipping along raceways. These effects cause high frequency vibrations to be generated.

It should be noted that specific information concerning the bearing construction is required to calculate the exact characteristic frequencies. However, these characteristic race frequencies can be approximated for most bearing between six and twelve balls by

$$f_o = 0.4nf_{rm} \qquad (3.27)$$

$$f_i = 0.6nf_{rm}$$

This generalization allows for the definition of frequency bands where the bearing race frequencies are likely to be present without requiring explicit knowledge of the bearing dimensions. Therefore, it is possible to formulate an effective detection scheme which monitors the related stator current spectrum for bearing defects.

3.3.3 Categorizing Bearing Faults

Bearing faults are grouped in to one of two categories :Single point Defects and Generalized roughness[26,27]

3.3.3.1 Single point Defects

A single point defect is defined as single, localized defect on an otherwise relatively undamaged bearing surface. A common example is a pit or spall. A single point defect produces one of the four characteristic fault frequencies depending on which surface of the bearing contain the fault. These predictable frequency components typically appear in the machine vibration and are often reflected into the stator current. In spite of the name, a bearing can possess multiple single point defects.

3.3.3.2 Generalized Roughness

Generalized Roughness is a type of fault where the condition of a bearing surface has degraded considerably over large area and become rough, irregular, or deformed. This damage may or may not be visible to the unaided eye. Nevertheless, there is no localized defect to be identified as the fault; rather, larger areas of the bearing surface(s) have deteriorated. A common example is the overall surface roughness produced by a contamination or loss of lubricant. The effects produced by this type of fault are difficult to predict, and there is no characteristic fault frequencies for the current or vibration associated with this type of fault. Generalized roughness fault are common in industry, while they are often neglected in the research literature. However when a generalized roughness fault reaches an advanced stage and the bearing is near failure, the fault can typically be detected via the rudimentary techniques commonly employed in industry

The flow chart in figure 3.11 illustrates the effects of these two categories of faults and where their fault signature appears. From this figure it is evident that both types of faults directly affect the machine vibration, in different ways. These effects are often reflected into the stator current.

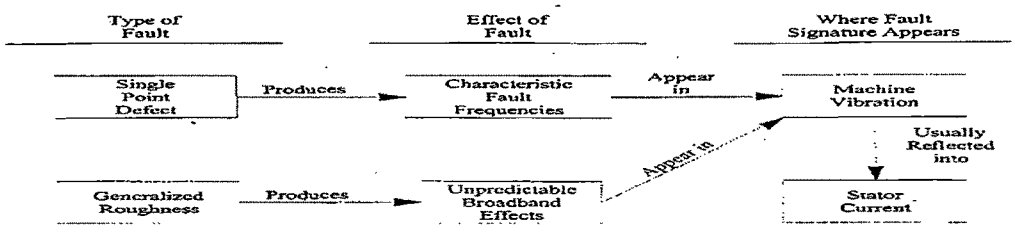

Figure 3.11 Flowchart showing the effects of two categories of faults and where their signature appears.

3.3.4 Results and Discussion

In order to the study effect of bearing vibrations to the stator current, a scarped bearing (6206), whose both inner and outer were damaged was mounted in driving end of motor. The outside diameter of the bearing was 62 mm and inside diameter of the bearing was 30mm. The pitch diameter was 46mm. The bearing was having 9 balls with an ball diameter of 9.525 mm. Assuming the contact angle of zero and motor operation at the rated shaft speed of 1428 rpm, the characteristic race frequencies were calculated and corresponding fault frequencies were calculated. The different frequencies are tabulated in table

Table 3.3 Characteristic Frequency for Bearing Faults

Sr. no.	Characteristic frequency	Value in Hz
1	fi	130
2	fo	84
3	f - fo	34
4	f + fo	134
5	f - fi	80
6	f + fi	180

Linear plot of the current spectrum recorded and processed is shown in figure 3.12. The frequency component produced by bearing defects was present in the spectrum. It is important to note that the frequency components produced by bearing defects are relatively small when compared to the rest of the current spectrum.

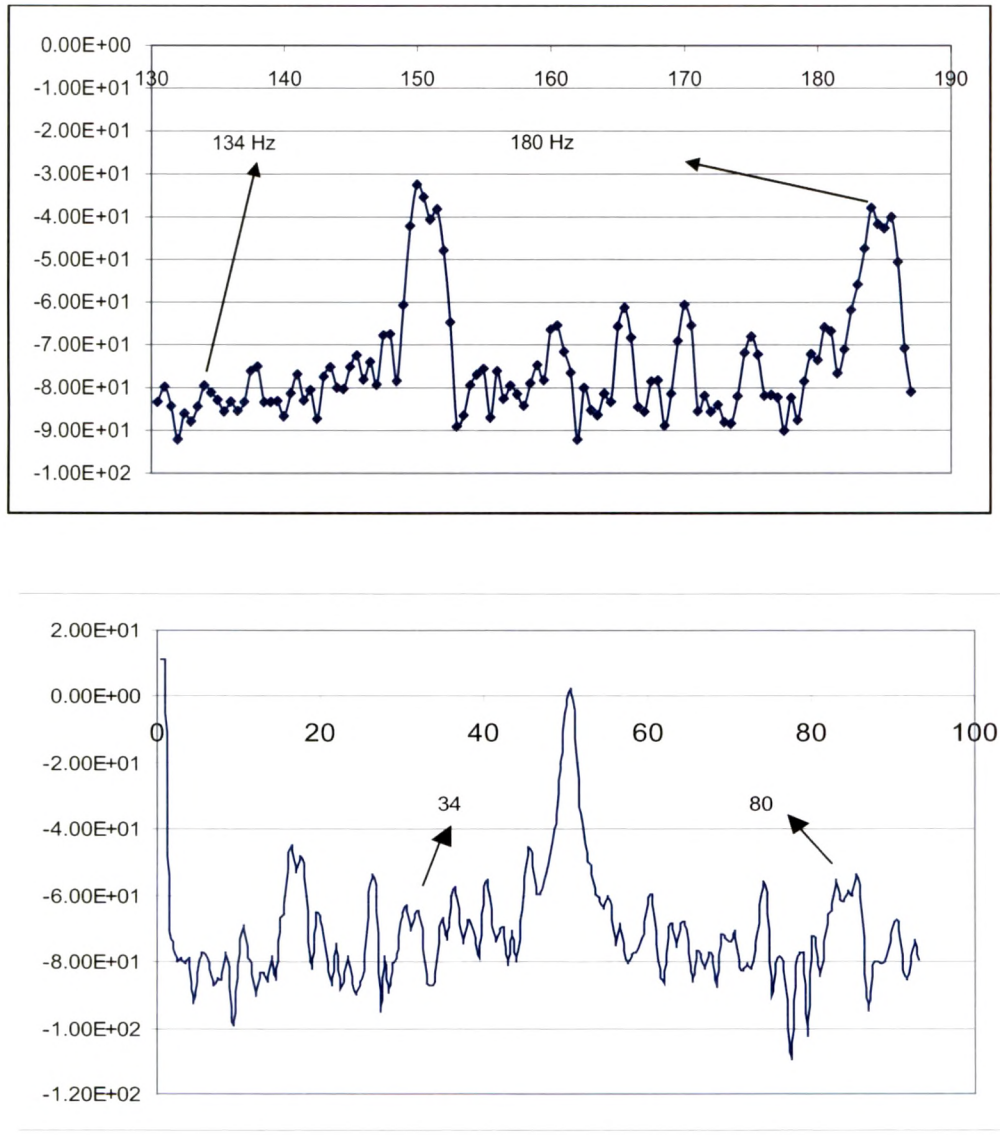

Figure 3.12: Peaks at characteristic frequencies for bearing faults

They fall at locations that are different from supply and slot harmonics of the machine. With spectral resolution, this discrimination makes the harmonics sufficiently distinct for use as effective diagnosis of rolling-element bearing damage

A single point defect will cause certain characteristic fault frequencies to appear in machine vibration; therefore there is one characteristic fault frequency associated with each of the four parts of the bearings. However generalized faults produces unpredictable (often broadband) changes in the machine vibration and hence stator current. Hence they can be detected only if the data is trended over a period of time.

3.4 Eccentricity Faults

3.4.1 Introduction to Eccentricity

Manufacturers take great care to ensure that air gap eccentricity is kept to minimum (e) (shown in figure 3.13) and typical maximum levels for a large induction motors are between 5 to 10% (i.e overall percentage air gap eccentricity-combination of static and dynamic).

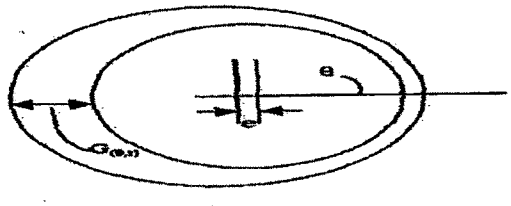

For static eccentricity: $G_{(\theta)} = G_m(1-E\cos\theta)$
For dynamic eccentricity: $G_{(\theta,t)} = G_m(1-E\cos(\theta-\omega_r t)$
where:
$G_{(\theta,t)}$ =length of airgap around the circumference
e =absolute eccentricity
G_m = nominal airgap length (as per motor specification)
$E = e/G_m$ = per unit airgap eccentricity or percentage
ω_r = rotational speed of rotor (rad/sec)
θ = angular distance around the airgap circumference

Figure 3.13: Air gap Eccentricity

There are two types of air gap eccentricity, namely static and dynamic in the former the minimum air gap is fixed and in the latter the minimum air gap revolves with the rotor. Figure 3.14 shows the two types of eccentricity

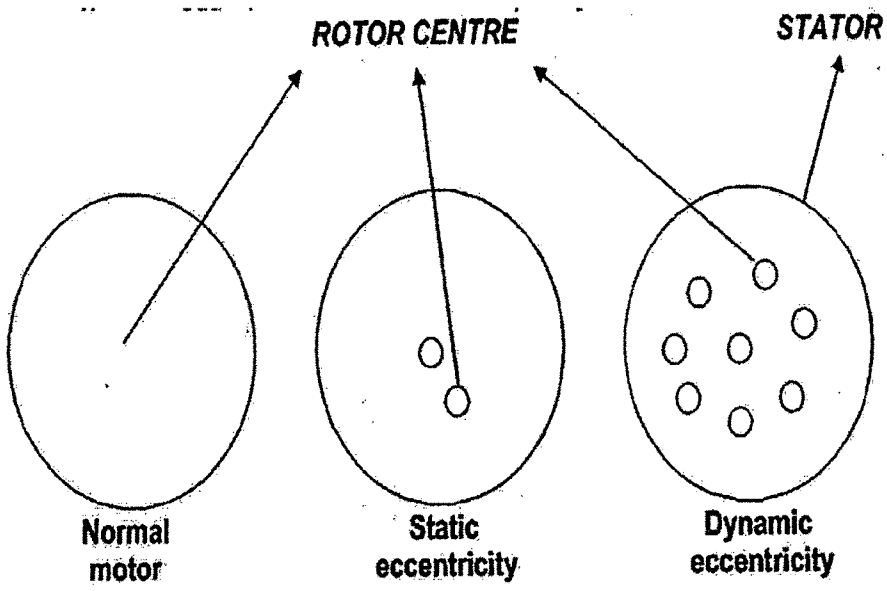

Figure 3.14: Static and Dynamic Eccentricity

3.4.2 Causes of Eccentricity

In practice there will always be an inherent level of both types present due to manufacturing tolerance. Manufacturers keep dynamic eccentricity as small as possible otherwise high levels of vibration will occur at the bearings. Apart from manufacturing tolerances, problems can still subsequently occur in practice and these include

Bearing wear can cause air gap eccentricity and this can be compounded since eccentricity will further increase the forces acting on the bearing and bearing failure can occur.

Following a repair or major overhaul the motor can be reinstalled with above normal levels for air gap eccentricity

In unusual cases thermal bowing of the shaft can cause dynamic eccentricity

Any increase in air gap eccentricity increases the electromagnetic forces acting on the stator core and windings and may lead to mechanical damage to the insulation. It is also known that acoustic noise level increase due to an increase in air gap eccentricity. A catastrophic failure can occur if the air gap eccentricity is at level such that the resultant unbalanced magnetic pull causes a rotor to stator rub. This can cause damage to the stator core and windings and a stator winding failure with consequential costly repair and lost production and income

The application of on line current monitoring to determine whether abnormal levels of air gap eccentricity can be diagnosed in large induction motors operating in industry has confirmed that it is possible to detect the problem and avoid a serious failure.

3.4.3 Diagnosis of Air gap Eccentricity

In practice, the operator requires a non invasive transducer to sense a signal with the minimum of disturbance to the running of the drive system. The use of current monitoring is proposed for detection of air gap eccentricity and following equation can be used to identify the frequency component in the current spectrum [19]

$$f_{ec} = f_1\left[\left(kR \pm n_d\right)\left(\frac{1-s}{p/2}\right) \pm n_\omega\right] \text{ where} \qquad (3.28)$$

R = no. of rotor bars. P= number of poles, s= slip

n_w = 1,3,5….. , f_1 = supply frequency, n_d = dynamic eccentricity =1

This gives the rotor slotting effects on the induced stator emfs and currents. This function is valid for static eccentricity when nd= 0. If static eccentricity increases then the magnitude of the components attributable to static eccentricity should also increase. If dynamic eccentricity exists, then nd=1 and new components should appear. The air gap eccentricity can be detected using above equation but the identification of whether it was static or dynamic eccentricity proved to be inconclusive since a high static eccentricity also produced dynamic eccentricity. The air gap eccentricity can be detected using equation (3.28) but the identification of whether it is static or dynamic eccentricity proved to be inconclusive since a high static eccentricity also produced dynamic eccentricity. The interaction between flux waves which produce rotating force waves and hence vibration due to the presence of both static and dynamic eccentricity was not modeled in the derivation of equation (3.28). To detect the components in the current spectrum which are predicted from equation (3.28), it is necessary to reduce the magnitude of the main supply frequency component via a high pass filter prior to recording and analysis of the current signal.

So also the dynamic eccentricity can produce components given by following equation [20,21]

$$f_1 \pm kf_r \qquad (3.29)$$

The components at these frequencies are due to the combination of static and dynamic eccentricity with the magnitudes increasing with both static and dynamic eccentricity.

Classical theory states that the flux components due to only dynamic eccentricity (given by equation (3.29)) have waves of p ±1 pole pairs and will therefore induce current components in a p pole pair stator winding[21]. A Theoretical analysis to model interactions between static and dynamic eccentricity [25] proved that flux waves with p pole pairs can occur at the frequencies given by equation (3.29) due to air gap modulation of mmf waves caused by both types of eccentricity existing simultaneously. Hence these flux waves can induce currents at $f_1 \pm f_r$ in a p pole pair stator winding. Hence the frequency components in the current spectrum given by equation (28) are not only due to dynamic eccentricity but are function of both static and dynamic eccentricity.

The presence of rotor slot harmonics (also called the principle slot harmonics or PSH) and the other eccentricity related harmonics is absolutely essential for most of the sensor less adjustable speed induction motor drives schemes and diagnosis of eccentricity faults. The principal slot harmonics are given by equation (3.28) with $n_d = 0$, $n_w = 1$, $k=1$. When one of these harmonics is a multiple of three, it may not exist theoretically in the line current of a balanced three phase wire machine.

However, the harmonics as described by (3.28) are not present in the machine for all combinations of p and R. This is due to fact that only flux which can produce voltage in a three phase stator winding is one that has number of pole pairs that the winding itself may produce [21]. However in a squirrel cage a flux with any number of pole pairs can induce a voltage. To be precise, for a healthy machine to produce a

spectrum of principal slot harmonics, the pole pair number R±np (n the harmonic order number) should be equal to the pole pair number of the space harmonics produced by a phase of the stator winding. For example, with 35 stator slots, and full pitch three phase concentric winding and R =44, p= 2; one principal slot harmonic can be seen. The same winding with R =43 or R =42 should not ideally give any principal slot harmonics. However in presence of static or dynamic eccentricity the pole pair number changes from R±np to R±np±1. This will then introduce additional harmonics as given by(3.28) with only R= 43 and not with R =44 or R =42 for same fundamental pole pair. In fact, with R=42, the speed detection algorithm using PSH are likely to fail.

While when both static and dynamic eccentricity are present additional components given by (3.29)will be present in the stator current spectrum of any three phase irrespective of p & R. However, these additional components will give rise to other additional current spectrums at the same frequency points described by (3.28) for dynamic eccentricity related components [38].

In General, PSH components is only present when at R is given by

$R = 2p[3(m\pm q)\pm r]$, $m\pm q = 01,2,3.....$ r= 0 or 1. (3.30)

Static eccentricity components is only present when at R is given by

$R = 2p[3(m\pm q)\pm r]\pm 1$, $m\pm q = 01,2,3.....$ r= 0 or (3.31)

3.4.4 Experimental Test results

Figure 3.15 shows the spectral plot of the current drawn by motor. This is a spectral plot with no eccentricity introduced (or with inherent levels of eccentricity due to manufacturing tolerances).

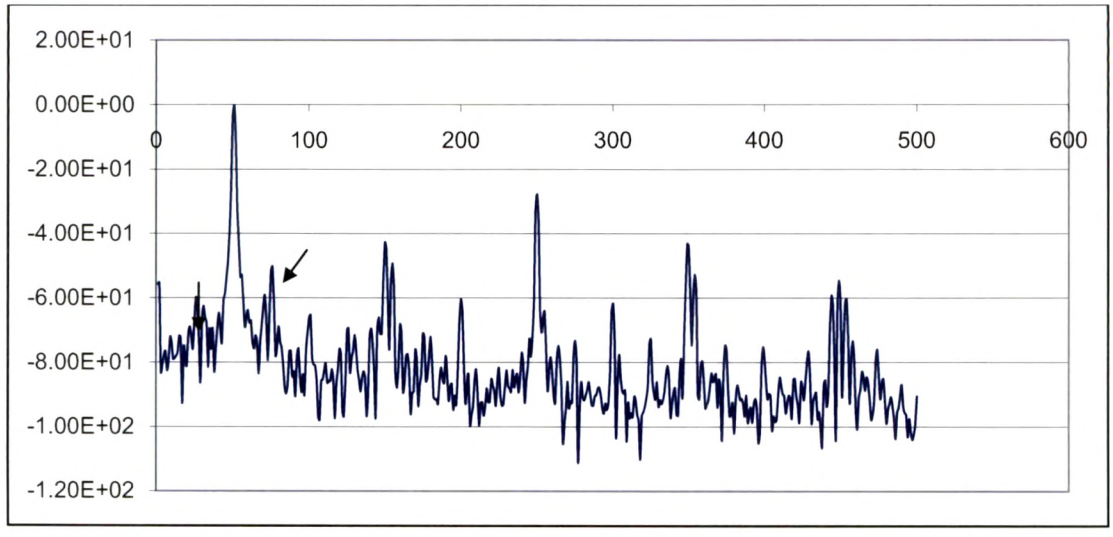

Figure 3.15: Current Spectrum with inherent level of eccentricity

The frequency components calculated from $f_1 \pm f_r$ (i.e 25 Hz and 75 Hz with f_1= 50hz and f_r = 25Hz) are having negligible magnitude. The frequency components related to static and dynamic eccentricity 398, 423 and 373 are of negligible magnitude. So also the magnitude dynamic eccentricity components 423 and 373 are different.

Figure 3.16 shows the spectral plot of the current drawn by motor, in which the static eccentricity was introduced by inserting the 0.1 mm thick strip on end shields. Table 3.4 shows the values of characteristic frequencies for eccentricity.

Table 3.4 Characteristic Frequencies for Eccentricity Fault

Rotor bars	14					
Speed	1492	rpm	Slip	0.005333		
Nw	1	-1	3	-3	5	-5
Se	398	298	498	198	598	98
Nd	1					
de	423	323	523	223	623	123
Nd	-1					
de	373	273	473	173	573	73

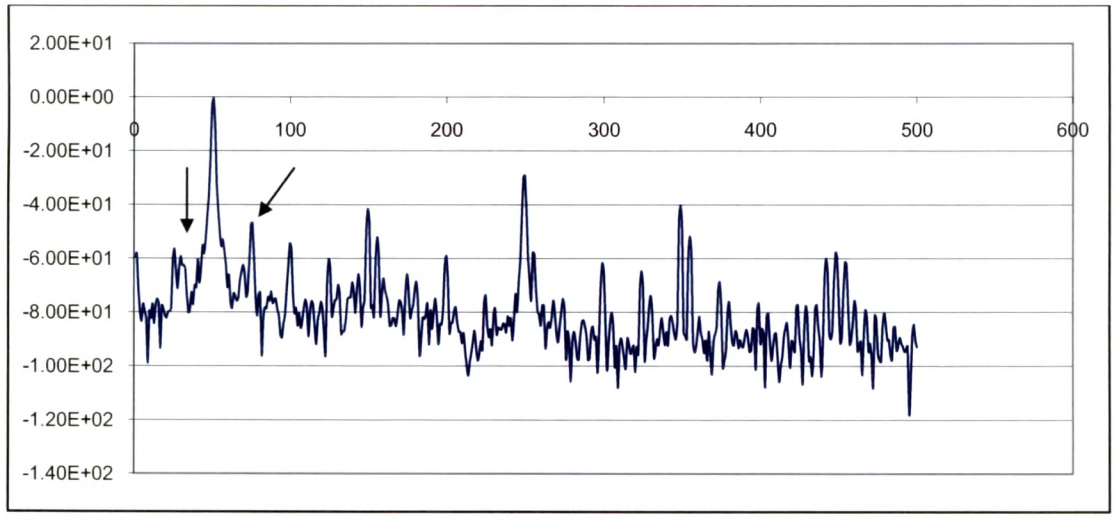

Figure 3.16: Current spectrum with eccentricity fault.

The magnitude of frequency component at 25 Hz and 75 Hz was increased by 10db. The frequency components related to dynamic and static eccentricity at 373 Hz, 398Hz and 423 Hz were also observed in the spectrum. The increase was from 5 to 6 db. The magnitude of dynamic eccentricity components at 373 and 423 Hz become equal pointing that there is eccentricity fault.

This means that severity of air gap eccentricity can be predicted by interpreting the current spectra for the above fault frequencies.

3.5 Stator Faults

3.5.1 Introduction

Stator winding failures are also a major problem in low and medium voltage induction motors. It should be noted that volume of low voltage motors is much greater than high voltage machines. In motors it is normally the case that insulation degradation cannot be initially diagnosed via on line measurements and the first indication of a problem will be that a fault actual develops. It is important to appreciate that there is clear distinction between insulation degradation prior to a fault and an actual fault. Stator winding faults can be classified as follows

1. Turn to turn short within coil – motor will continue to operate but for how long?
2. Short between coils of the same phase – motor can continue to operate but for how long?
3. Phase to phase short – motor fails and protection equipment disconnects the supply
4. Phase to earth short – Motor fails and protection equipment disconnects the supply
5. Open circuit in on phase (Single Phasing) – motor may continue to operate depending on the load condition and protection equipment.

Pre warning of serious problem (3 and 4 above) can only be achieved if shorted turns within coil (one or two shorted turns) can be initially diagnosed via online

diagnostic techniques. This requires continuous online monitoring to diagnose the faults state in 1 and 2 above.

There is also the question of how long does it take for shorted turns within coil to develop into phase to phase or phase to earth fault and motor failure? This question has not been resolved and will be function of many variables and will in fact be unique to each motor. Some operators and manufacturers have previously considered that it is not worth diagnosing shorted turns or coils in stator windings since the lead time to failure is too short to merit a continuous online diagnostic system. The concept that the motor has already developed a fault and will need to be repaired has prevailed. This philosophy is generally now considered to be somewhat out dated and defeatist. In modern production process any lead time can be extremely advantageous since unexpected failure of a drive can be very costly and in some industries it can also be a serious safety hazard. If shorted turns in a stator coil can be diagnosed a preplanned shut down can be arranged for the motor to be replaced by healthy one and the faulty one sent for repair.

With respect to the problem of single phasing it is relatively easy to diagnose the problem provided the correct protection equipment is used to cater for all load conditions. It is also possible to monitor and analyze signals such as current to diagnose single phasing under any load operating condition.

3.5.2 Diagnosis of Stator faults

For ideal machine the axial leakage flux is zero. This is because, under fault free conditions, the rotor and stator currents should be perfectly balanced. The occurrence of fault on the motor results in a change in the air gap space harmonics

distribution. The space harmonic distribution of mmf due to balanced, full pitched, three phase winding fed from balanced supply frequency w is given by [28,29]

$M=0.955N_1\{k_{w1}\cos(\omega t-p\theta) + 0.2k_{w5}\cos(\omega t+5p\theta)-0.14k_{w7}\cos(\omega t-7p\theta)\ldots(3.32)$

Where k_{wn} is the nth winding factor

p is number of pole pairs,

θ is the angular displacement from the stator datum

This represents a rotating set of harmonics of order $6n\pm1$ which can be simplified to the corresponding air gap fluxes [28, 29]

$Bs = B_1\cos(\omega t-p\theta) + B_5\cos(\omega t+5p\theta)+B_7\cos(\omega t-7p\theta)\ldots.$ (3.32.1)

Where Bn is the spatial harmonic flux

This expression is in the stator frame of reference. Consequently, because the shaft flux or the rotor is of interest, it is necessary to refer to equation (3.32.1) to the rotor reference frame. Consider the situation in which β is the angular displacement between the rotor and stator datum positions, and α is defined to be the angular displacement from the rotor datum. Then $\theta= \alpha+\beta$

If the angular rotor speed is ω_r then

$\theta= \alpha + \omega_r t$ (3.33)

Now using the normal expression for the slip of the motor, i.e

$S= (\omega_s- \omega_r)/ \omega_s$ where ω_s the synchronous speed $= \omega / p$

$\omega_r = \omega (1-s)/p$ (3.34)

In general

$B_{ns} = B_n\cos(\omega t\pm p\theta)$ (3.35)

Substituting equation (3.33) & (3.34) into (3.35) leads to

$$B_{ns} = B_n \cos\{1 \pm n(1-s)\,\omega t \pm np\alpha\} \qquad (3.36)$$

Equation (3.36) gives the frequency components of the current that are induced in the rotor due to the air gap space harmonics of a balanced winding and supply. In addition to these harmonics, the fundamental of the supply frequency will also appear in the axial flux spectrum. The presence of additional, higher order harmonics can be accounted for by using n ω rather than ω

The effect of the inter turn fault is to remove a turn from the stator winding. This will have a small, but finite, effect on the main air gap flux distribution. In addition, an emf will be induced in the shorted turn which will result in a current flow limited only by the self impedance of the fault. This impedance essentially determines the transition time between turn and ground wall insulation failure.

The fault current due to the shorted turn is the source of an additional mmf pulse, which also has a space harmonics distribution which is superposed on the main field distribution. This will lead to a change in the time harmonics observed in the current.

Adding in supply time harmonics of higher order k , leads to the completely general expression and with mark space ration of 1 : (2p-1) causing every $2p^{th}$ harmonic to be absent.

$$B_{ns} = B_n \cos\{1 \pm n(1-s)\omega t \pm np\alpha\} \quad , n \neq 2pm, \text{ all } m$$

The key element of this expression is

$$[k \pm n(1-s)/p]f \qquad (3.37)$$

For k = 1,3,5 and n =1,2,3...(2p-1)

However based on the experimental results [27] only certain current components are selected from the classical theory to ensure the reliable diagnosis of shorted turn. Mainly components corresponding to k=1, n=3 and k=1, n=5 are good indicators of shorted turns in low voltage motors 2pole and 4 pole.

Another classical theory based on the rotating wave approach [12] gives the indication about the shorted turns in induction motors. The objective here is effectively to use the stator winding itself as the sensor for the detection of abnormalities in the windings. The harmonics which are expected to vary and which have their origin in the stator currents are given as

$$fsc = f_1\left[(jrtR)\left(\frac{1-s}{p}\right) \pm 2jsa \pm ist\right] \tag{3.38}$$

and the harmonics expected to vary and which have their origin in the rotor currents are

$$frc = f_1\left[(jrtR \pm K)\left(\frac{1-s}{p}\right) \pm 2jsa \pm irts\right] \tag{3.39}$$

where R= no. of Rotor bars

i,j,k are integers

s= slip

p= pair of poles

It is shown that [12] most reliable indicators of the presence of the fault are the lower side band of field rotational frequency with respect to the fundamental together with some of the components that are related to slotting.

3.5.3 Experimental Test results

A series of tests were conducted on specially designed test rigs on which fault could be introduced. Figure 3.17 shows schematic representation of machine operating as wye connected induction motor.

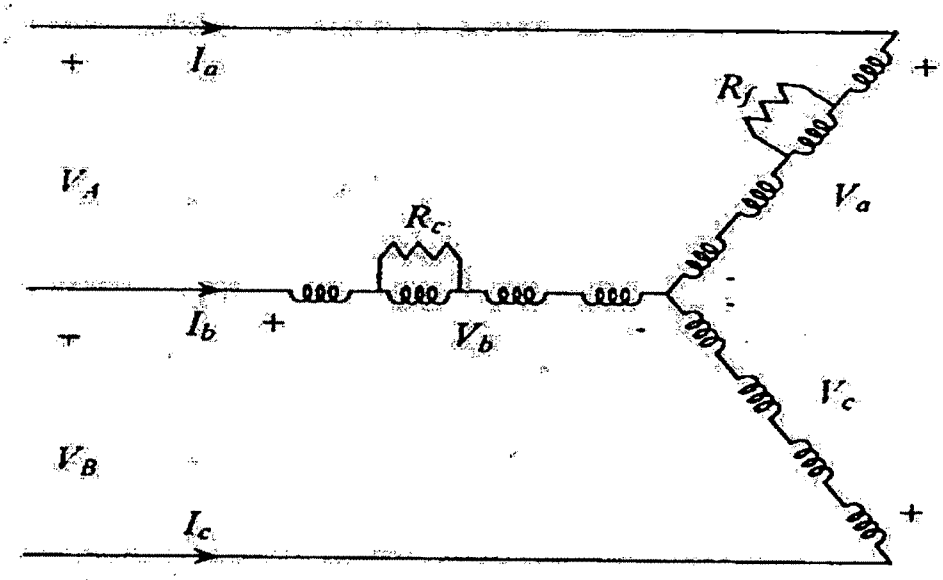

Figure 3.17: Schematic diagram of the laboratory machine

The Photograph of the machine used for experiment is as shown below

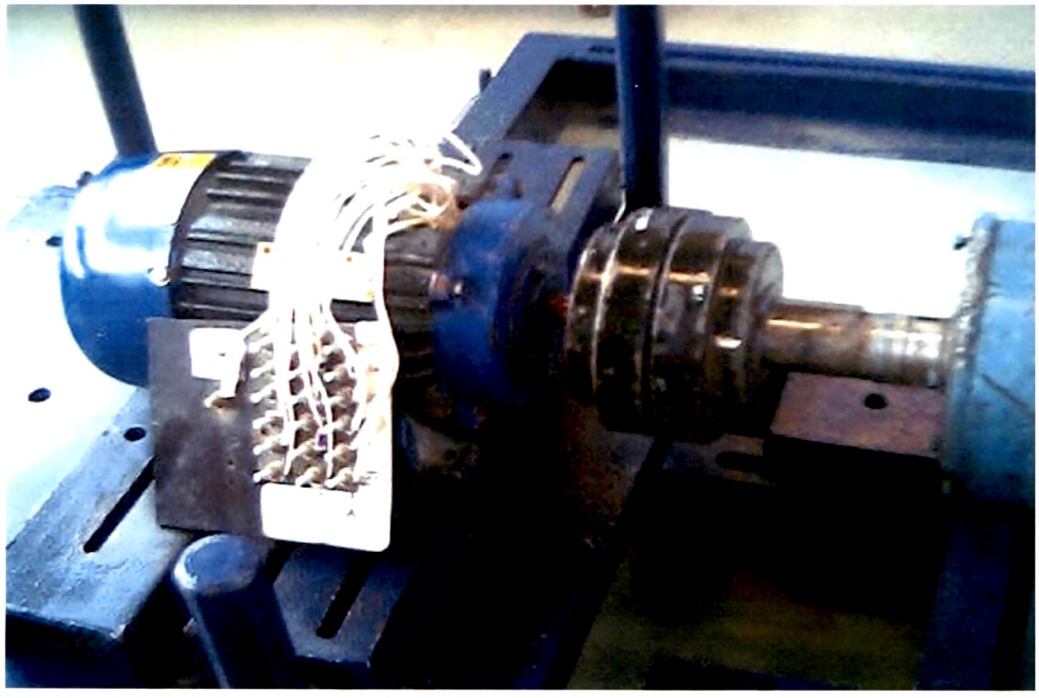

Photograph 3.1: Induction motor rewounded with tapings at 1,3,5,20,25 turns

The winding arrangement of this machine is such that the inter turn fault can be introduced in this. The inter turn short circuit is controlled with variable resistor and was introduced in B phase.

Inspection revealed that rotor of the test machine possesses 18 slots. Taking account of the principal slot component only, first and third time supply harmonics and the main saturation modulation, from above equation, we expect, in addition to usual odd harmonics at 50, 150, 250, 350...Hz, the following 198, 298,398,498,598 components around the principal slot components for s= 0.001 will appear.

It was found that for the 2 turn inter turn short circuit, frequency component 398 was most sensitive to fault. From no fault to maximum fault current variations in the range of 49% was recorded. Components 498 Hz were found to be less sensitive. The component 198 and 298 Hz was decreasing in all the phases. But decreasing being more pronounced in the faulty phase.

For 4 turn inter turn short circuit, frequency component 398 Hz also increased from no fault conditions. The variations of more than 100% were observed from no fault to maximum fault current.

For 20 turn inter turn short circuit, frequency component 398Hz also increased. The variation of more than 400% was observed from no fault to maximum fault current.

From the experiments it was apparent that some of the specified frequency components were redundant, but whether or not this would be the case for other machines and for the same harmonics requires further investigations.

Figure 3.18, 3.19, shows the variations of different frequency components for 2 turn, 4 turn and 20 turn inter turn short circuit.

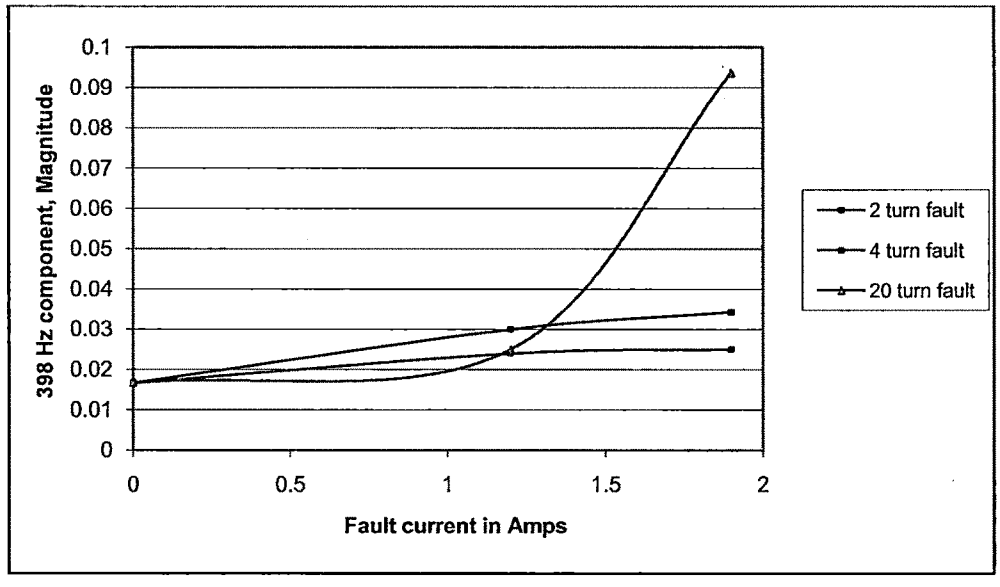

Figure 3.18: Variation of 398 Hz component with respect to fault

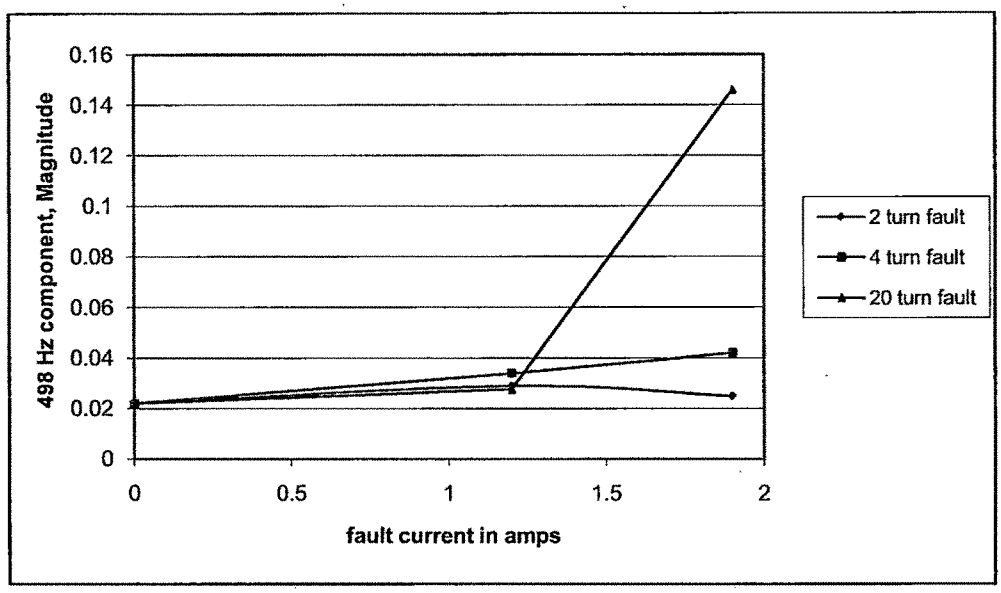

Figure 3.19 : Variation of 498 Hz component with respect to Fault current

3.5.4 Inverter Fed Motors

Motors which are fed from Inverter will already have the higher content of time harmonics. These time harmonics will can be identified by taking the voltage signature. Hence for Inverter fed motors the voltage signature is taken first and all the time harmonics are identified. Based on this data, these harmonics are extracted from the current signature. After all time harmonics appearing the voltage signature are extracted then the analysis presented in the section 3.5.2 are applied to diagnose the stator winding faults for inverter fed motors.

3.6 CONCLUSION

1) Broken Rotor Bars

It is shown that presence of rotor faults such as bar failure, end ring failure or joint failure between bar and ring can be detected by current monitoring. The presence of side band LSB1 gives the indication of rotor faults. The magnitude of side band gives the amount of failure in the rotor. The increase in core losses and the load current also gives the indication of some problem with the rotor. With each failure in bar the efficiency and speed of the motor also decreases. It can be concluded that the online current monitoring can pin point the problem with the rotor faults. The increase in core losses and load current, subsequent decrease in efficiency and speed with each bar failure can also be used to detect the rotor faults.

The magnitude of the line frequency sidebands due to asymmetries may be comparable to or larger than those due to a broken bar in the same motor. However the magnitudes of the asymmetry components decay much more rapidly, in the higher harmonics, than those for a broken bar

The stator current is affected by load torque oscillations in a way similar to that explained above. In the sinusoidal steady state, it is clear that load torque oscillations produce an oscillation in the developed torque T. Therefore, since the mechanical system is assumed linear, the torque developed by an induction motor contains all the frequency components of the load torque. The magnitude of the developed torque harmonics is primarily dependent on the system inertia.

The impact of the load on a fault detection scheme is also dependent on the mechanical system inertia. In many cases, the load oscillation is heavily damped in the developed torque due to high inertia. In many cases, the load oscillation is

heavily damped in the developed torque due to high inertia. In this situation, adequate detection can be accomplished by monitoring fault frequencies at sufficiently high harmonics.

2) Bearing Degradation

From the experimental results, it has been shown that there is feasibility of detecting the bearing faults using a spectrum of single phase of stator current of an induction motor. Since rolling element bearings support the rotor, bearing defect also produces variations in the air gap of the machine. These variations generate the noticeable effect in the current spectrum. The predictability of the air gap frequencies has been extended to include faults in rolling element bearings.

The magnitude of these faults frequencies being relatively small when compared to the rest of current spectrum, but they fall at locations that are different from supply harmonics and slot harmonics of the machine. With good spectral resolution, this discrimination makes the fault harmonics sufficiently distinct for use as effective detection of rolling element bearing damage.

The fault frequencies depend upon the construction and dimension of the bearings installed. Hence it requires the knowledge of the bearing dimension and construction.

A single point defect will cause certain characteristic fault frequencies to appear in machine vibration; therefore there is one characteristic fault frequency associated with each of the four parts of the bearings. However generalized faults produces

unpredictable (often broadband) changes in the machine vibration and hence stator current. Hence they can be detected only if the data is trended over a period of time

3) Eccentricity Faults

The combination of interpreting the current spectra in two distinctly different frequency bands to identify components which are a function of static and dynamic eccentricity has proved to be reliable method for detecting the existence of abnormal levels of air gap eccentricity particularly in large induction motors.

The two distinct frequency bands are; one in the region of f1±fr and another in the region of rotor slot harmonics.

The frequency components in the current spectrum given by equation f1±fr are not only due to dynamic eccentricity but are function of both static and dynamic eccentricity. While the frequency components in the range of rotor slot harmonics can be identified the dynamic or static eccentricity.

The harmonics as described by rotor slot harmonics are not present in the machine for all combinations of p and R. In General, PSH components is only present when at R is given by

$R = 2p[3(m\pm q)\pm r]$, $m\pm q = 01,2,3.....$ $r= 0$ or 1.

Static eccentricity components is only present when at R is given by

$R = 2p[3(m\pm q)\pm r]\pm 1$, $m\pm q = 01,2,3.....$ $r= 0$ or

4) Stator Winding Faults

From the experimental results, it is verified that the presence of stator inter trun fault changes the current spectrum particularly some of the slot harmonics. The monitoring of variations in the slot harmonics in the current spectrum can detect the stator inter turn fault. Magnitude of some of the components may increase and some of components may reduce. Hence the trending of data is required.

However based on the experimental results only certain current components are selected from the classical theory to ensure the reliable diagnosis of shorted turn. Mainly components corresponding to k=1, n=3 and k=1, n=5 are good indicators of shorted turns in low voltage motors 2pole and 4 pole.